


# MODELING OF TRANSPORT CONTAMINANTS MOVEMENT IN A GEOTHERMAL REINJECTION SYSTEM

by

612300  
**ANDREA E. SERVIÑO**

*A thesis submitted in partial fulfilment of the requirements for the degree  
of Master of Science in Chemical Engineering*



College of Engineering  
De La Salle University

April 1995

## ABSTRACT

A simulation technique has been developed to assess the impact of shallow reinjection of geothermal wastewater at Palinpinon field to the surrounding groundwater resources. The physical model assumes single fracture connecting the reinjection and the groundwater wells. Using the analytical solutions of the resulting coupled dispersion-advection equation for the fracture flow and the diffusion equation for the flow into the rock matrix, relative concentrations of chloride at various points within the fracture and at observation points 4000 and 2000 meters away are calculated. For porosities of 0.03 to 0.1 which is typical for welded tuffs and clay alteration products which are the dominant rocks in the area, matrix diffusion was found to be an efficient retardation mechanism for the dispersion of the waste fluids.

Boron dispersion was also modeled by taking into account its probable adsorption into clays. Using reasonable estimates for the retardation coefficients for boron, adsorption may delay its breakthrough by up to 100 days.

A general program coded in FORTRAN 77 has also been developed to evaluate the general transient solutions of the mass transport equations in fractured porous media. The method employed in the evaluation is the Gauss-Legendre quadrature. The technique provides insights into the gross behavior of reinjected fluids by putting constraints on breakthrough times, relative concentrations of the contaminant along the fracture and within the matrix and matrix retention of contaminants.

## NOTATION

### Transport Parameters:

$c_f, c$	[M/L <sup>3</sup> ]		Concentration in the fracture.
$c_m, c'$	[M/L <sup>3</sup> ]		Concentration in the matrix.
$c_o$	[M/L <sup>3</sup> ]		Input concentration.
$c/c_o$			Relative concentration.
$q$	[M/L <sup>2</sup> T]		Diffusive flux perpendicular to the fracture axis.
$V$	[L/T]	V	The velocity of water in the fracture.
$\alpha_L$	[L]	AL	The value of the longitudinal dispersion in the direction of the flow.
$R$		R	Face retardation coefficient.
$\tau$		TAU	Matrix tortuosity.
$D^*$	[L <sup>2</sup> /T]	DASTX	Free water molecular diffusion coefficient.
$2b$	[L]	FW	Fracture width.
$\theta$		PORS	Matrix porosity.
$R'$		RPRIM	Matrix retardation coefficient.
$x$	[L]	X	Coordinate along the fracture axis.
$\lambda$	[1/T]	XLAMDA	Decay constant equivalent to $\ln 2/t_{1/2}$ .
$t$	[T]	T	Time.
$y$	[L]	YM	Direction adjacent to the fracture.

### Other Parameters:

$$Y' = \frac{v^2 \beta^2 x^2}{4A\xi^2} + B(y - b)$$

$$B = (R'/D')^{1/2}$$

$$T' = \left( t - \frac{Rx}{V} \right)^{1/2}$$

$$W = \frac{Rx}{VA} + B(y - b)$$

### SFTM Implementation

#### Main Program

$a$ and $b$	F,S	Integration limits.
$c/c_0$	CONC	Calculated value of the relative concentrations.
	M	Number of points for the Gauss-Legendre formula.

#### Function FRACT

$\xi$	XI	Integration variable of the general analytical solution.
$D'$	[L <sup>2</sup> /T] HD	Hydrodynamic dispersion $D' = \alpha_L + D^*$ .
$v$	XNU	$v = V/2D$ .
$\eta$	ETA	$\eta = \frac{\lambda R}{4D\xi^2}$ .
$\beta^2$	.BSQRD	$\beta^2 = \frac{4RD}{V^2}$ .
$D'$	[L <sup>2</sup> /T] DPRIM	$D' = \tau D^*$
$A$	A	$A = \frac{bR}{\theta(R'D')^{1/2}}$ .
$Y$	YBAR	$Y = \frac{v^2 \beta^2 x^2}{4A\xi^2}$
$T$	TBAR	$T = \left( t - \frac{Rx^2}{4D\xi^2} \right)^{1/2}$

### **Function GAUSS**

<i>c</i>	C	$c = (b-a)/2$
<i>d</i>	D	$d = (b+a)/2$
<i>i</i>	I	Subscript for vectors <i>p</i> and <i>k</i> .
<i>j</i>	J	Index on the repeated sum of Eq. (4.7).
	JFIRST	Initial value of <i>j</i> , <i>k<sub>i</sub></i> .
	JLAST	Final value of <i>j</i> , <i>k<sub>i+1</sub></i> -1.
	KEY	Vector <i>k</i> .
	NPOINT	Vector <i>p</i> .
	SUM	Repeated sum of Eq. (4.7).
	WEIGHT	Vector of weight factors, <i>w<sub>j</sub></i> .
	Z	Vector of Legendre polynomial roots, <i>z<sub>j</sub></i> .

### **Function ERFC**

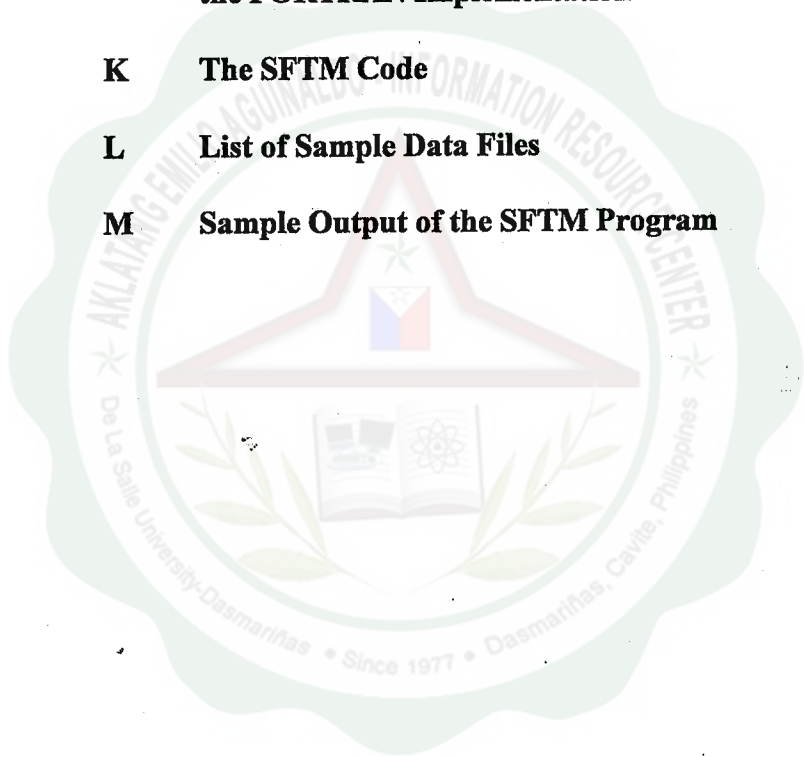
Y	Y	Dummy argument of the complementary error function defined as erfc(Y).
---	---	--

# TABLE OF CONTENTS

		<i>Page No.</i>
	<b>ABSTRACT</b>	i
	<b>ACKNOWLEDGEMENTS</b>	ii
	<b>NOTATION</b>	iii
	<b>TABLE OF CONTENTS</b>	vi
	<b>LIST OF FIGURES</b>	ix
<b>Chapter 1</b>	<b>INTRODUCTION</b>	1
	1.1 Background of the Study	1
	1.2 Objectives of the Study	2
	1.3 Significance of the Study	3
	1.4 Scope and Limitations	3
<b>Chapter 2</b>	<b>REVIEW OF LITERATURE</b>	5
	2.1 Transfer Mechanisms	5
	2.2 Flow in Fractured Media	9
	2.3 Levels of Mathematical Transport Modeling	11
<b>Chapter 3</b>	<b>CONTAMINANT TRANSPORT IN FRACTURED POROUS MEDIA: ANALYTICAL SOLUTIONS FOR A SINGLE FRACTURE</b>	15
	3.1 Model Description	15
	3.2 Analytical Solutions to Contaminant Transport	16
	3.2.1 Transport of a Non-reactive Solute	16
	3.2.2 Transport of a Reactive and Adsorbing Solute	20
	<i>The General Transient Solution</i>	22
	<i>Transient Solution for the Special case <math>D=0</math></i>	23
	3.3 Model Calculation Methods	25
	3.3.1 Method of Evaluation of the Simplest Solution	25

	<b>3.3.2 Method of Evaluation of the General Transient Solution</b>	<b>27</b>
<b>Chapter 4</b>	<b>NUMERICAL INTEGRATION OF THE GENERAL ANALYTICAL SOLUTION</b>	<b>29</b>
	<b>4.1 The Method of Gaussian Integration</b>	<b>29</b>
	<b>4.2 FORTRAN Implementation of the Gaussian Integration</b>	<b>30</b>
	<b>4.2.1 Method of Solutions</b>	<b>30</b>
	<b>4.2.2 SFTM Program Structure</b>	<b>34</b>
	<b>4.3 Results and Discussion</b>	<b>35</b>
	<b>4.4 Summary and Conclusions</b>	<b>37</b>
<b>Chapter 5</b>	<b>PALINPINON CASE : A FIELD APPLICATION</b>	<b>43</b>
	<b>5.1 Statement of the Problem</b>	<b>43</b>
	<b>5.2 Chloride Modeling Results</b>	<b>48</b>
	<b>5.3 Boron Modeling Results</b>	<b>60</b>
<b>Chapter 6</b>	<b>SUMMARY AND CONCLUSIONS</b>	<b>66</b>
	<b>REFERENCES CITED</b>	<b>68</b>
	<b>APPENDICES</b>	
	<b>A Derivation of the Simple Analytical Solution</b>	<b>71</b>
	<b>B Derivation of the General Transient Solution and for the Case <math>D=0</math></b>	<b>76</b>
	<b>C Spreadsheet Calculation of Breakthrough Times in the Fracture</b>	<b>87</b>
	<b>D Spreadsheet Calculation of Breakthrough Times From the Fracture Into the Matrix</b>	<b>89</b>
	<b>E Spreadsheet Calculation of Concentration Distribution Along the Fracture</b>	<b>91</b>
	<b>F Spreadsheet Calculation of Penetration Distance Into the Matrix</b>	<b>93</b>

<b>G</b>	<b>Spreadsheet Calculation of the Behavior of the Integrand of the General Analytical Solution</b>	<b>95</b>
<b>H</b>	<b>Spreadsheet Calculation of the Lower Integrating Limits for <math>t</math>-Variables</b>	<b>97</b>
<b>I</b>	<b>Spreadsheet Calculation of the Lower Integrating Limits for <math>x</math>-Variables</b>	<b>98</b>
<b>J</b>	<b>Numerical Integration of a 15-Point Gauss-Legendre Formula using Spreadsheet-Based Procedure to Validate the FORTRAN Implementation</b>	<b>99</b>
<b>K</b>	<b>The SFTM Code</b>	<b>101</b>
<b>L</b>	<b>List of Sample Data Files</b>	<b>107</b>
<b>M</b>	<b>Sample Output of the SFTM Program</b>	<b>108</b>





## LIST OF FIGURES

Page No.

<b>Fig. 1.1</b>	Map of the Palinpinon-1 production field showing location of production and reinjection wells. Mapped geologic structures are also shown. The deviated production wells are designated by "D". Reinjection wells possess "R" in their designations.	4
<b>Fig. 2.1</b>	Schematic diagram showing the essential features of (a) plug flow, (b) plug flow accompanied by longitudinal dispersion, and (c) plug flow accompanied by transverse dispersion.	7
<b>Fig. 2.2</b>	An illustration of a single fractured porous model.	14
<b>Fig. 3.1</b>	Fracture-Matrix model.	16
<b>Fig. 3.2</b>	Transport through volume element. An example of a flat-slab geometry.	17
<b>Fig. 4.1</b>	Typical integrands for the general analytical solution, high velocity case and no decay (at $t = 100$ days).	39
<b>Fig. 4.2</b>	Typical integrands for the general analytical solution, high velocity case and no decay (at $t = 10000$ days).	39
<b>Fig. 4.3</b>	Typical integrands for the general analytical solution, low velocity case and no decay.	40
<b>Fig. 4.4</b>	Concentration distribution along the fracture at various times.	41
<b>Fig. 4.5</b>	Contaminant breakthrough curves at 500 m from the source for matrix porosities of 0.03 and 0.1.	42
<b>Fig. 5.1</b>	Structural map of N-1 and the monitoring stations.	46
<b>Fig. 5.2</b>	Flow profile from Ticala down to the lower watershed.	47

<b>Fig. 5.3</b>	Chloride breakthrough curves at well 5538 for an initial Cl concentration of 15000 ppm.	50
<b>Fig. 5.4</b>	Chloride breakthrough curves at well 5538 for matrix porosities of 0.03 and 0.1.	51
<b>Fig. 5.5</b>	Chloride concentration profiles along the fracture between N-1 and well 5538.	52
<b>Fig. 5.6</b>	Chloride concentration profiles from the fracture into the matrix at x-distances of 0,2000,4000 m from N-1 (for an initial Cl concentration of 15000 ppm).	53
<b>Fig. 5.7</b>	The effect of the magnitude of chloride diffusion coefficient $D^*$ to the breakthrough curve (for an initial Cl concentration of 15000 ppm)	54
<b>Fig. 5.8</b>	Chloride breakthrough curves at well 5544 for an initial Cl concentration of 15000 ppm.	56
<b>Fig. 5.9</b>	Chloride breakthrough curves at 2000 m from N-1 for matrix porosities of 0.03 and 0.1.	57
<b>Fig. 5.10</b>	Chloride breakthrough curves from the fracture into the matrix for an initial Cl concentration of 15000 ppm.	58
<b>Fig. 5.11</b>	Effect of matrix porosities on the contaminant breakthrough curves.	59
<b>Fig. 5.12</b>	Boron breakthrough curves at well 5538 for an initial boron concentration of 72 ppm.	62
<b>Fig. 5.13</b>	Concentration profiles of boron at well 5538 for an initial boron concentration of 72 ppm.	63
<b>Fig. 5.14</b>	Boron breakthrough curves from the fracture into the matrix for an initial boron concentration of 72 ppm.	64
<b>Fig. 5.15</b>	Concentration profiles of boron from the fracture into the matrix for an initial boron concentration of 72 ppm.	65